A High Performance Single-Domain LCD With Wide Luminance Distribution

Yating Gao, Zhenyue Luo, Ruidong Zhu, Qi Hong, Shin-Tson Wu, *Fellow, IEEE*, Ming-Chun Li, Seok-Lyul Lee, and Wen-Ching Tsai

(Invited Paper)

***Abstract*—In this paper, we review the device structures and present the simulation results of four single-domain LCDs with a quasi-collimated backlight and a free-form optics-engineered diffuser. Such a non-emissive LCD exhibits similar luminance distribution to an emissive OLED, while keeping high transmittance, high contrast ratio over a large (80°) viewing cone, with low ambient reflection, indistinguishable color shift, and negligible off-axis grayscale distortion.**

***Index Terms*—Fringe field switching, in-plane switching, liquid crystal display (LCD), OLED-like luminance distribution, single domain.**

I. Introduction

RECENTLY, "LCD or OLED: who wins?" is a hot debatable topic [1], [2]. Liquid crystal display (LCD) has advantages in long lifetime, low power consumption, high resolution density, and low cost; comparable performance with OLED (organic light emitting diode) in ambient contrast ratio, color gamut (with quantum-dot backlight), and thin profile, but disadvantages in flexibility, true black state, and response time. However, one important feature of OLED which is often neglected by the LCD camp is its much broader luminance distribution due to its emissive nature [3]. This might not be a great advantage in cell phones or other display devices intended for single user, but can be very favorable for large screen displays where multiple viewers can enjoy the display from different angles. Therefore, introducing high performance LCD with wide luminance distribution (OLED-like or even Lambertian) is necessary.

Several factors contribute to the relatively narrow luminance distribution of a LCD. First of all, LC is a non-emissive material, so that it requires a backlight unit to illuminate the displayed images. In typical LCDs, the luminance distribution of backlight has a FWHM (full width at half maximum) less than 60°. Taking iPhone 6 and iPhone 5 as examples, at 30° viewing angle the screen brightness drops to 40% for iPhone 5 and to 56% for iPhone 6 [4]. The viewing angle problem is not just diminished brightness, but also reduced contrast ratio and degraded color gamut, which is referred to as off-axis image distortion [5]. These problems originate from different phase retardation of the LC layer between on-axis and off-axis. The LC layer is usually optimized at normal viewing direction, so that at dark state there is either no phase retardation (for in-plane switching (IPS), fringe field switching (FFS) and vertical alignment (VA) modes) or maximum polarization rotation effect (twisted nematic (TN) mode) for normal incident light. But at oblique angles, the incident light experiences different phase retardation because of the anisotropic refractive index ellipsoid of the LC mediums. As a result, the light would partially leak through the crossed analyzer and renders a poor dark state. The same goes for bright states, leading to color washout and color shift at a large viewing angle.

Extensive efforts [6]–[11] have been devoted to solving the viewing angle problem. These approaches can be categorized into three groups: 1) laminating a compensation film externally to an LCD panel; 2) modifying the internal device structure by creating multiple domains toward different directions; and 3) combination of both. Nowadays, film-compensated multi-domain structure is the common approach. The basic idea of phase compensation is to use an anisotropic optical film (or multiple films) to balance the extra or insufficient phase retardation caused by the LC layer and the light leakage of crossed polarizers at oblique angles. For example, the phase compensation films developed by Fuji Photo [12]–[14] and Samsung [15] are quite effective for TN and VA LCDs. There are also compensation films for blue phase [16] and IPS [17] LCDs. A more comprehensive review on uniaxial-film compensated LCDs was presented in [11]. By adopting compensation films, one can enlarge the central viewing cone, but it is still difficult to achieve high contrast at large angles.

In a multi-domain LCD [18]–[23], each pixel is divided into several sub-pixels that contain patterned electrodes (usually zigzag shape) and molecular alignment directions. On a macroscopic scale, the optical anisotropies in different domains compensate for each other, so that the image quality is less dependent on the viewing angle, as compared to a single-domain LCD. This approach is especially advantageous at large viewing angle. However, the transmittance of a multi-domain LCD is lowered due to disclination lines at domain boundaries.

In this paper, we focus on another promising solution, though not prevalently adopted, utilizing a quasi-collimated backlight

Manuscript received January 28, 2015; revised February 26, 2015; accepted February 26, 2015. Date of publication March 13, 2015; date of current version March 24, 2015. This work is supported by AU Optronics, Taiwan.

Y. Gao, Z. Luo, R. Zhu, Q. Hong, and S.-T. Wu are with the College of Optics and Photonics, University of Central Florida, Orlando, FL 32816 USA (e-mail: yating_gao@knights.ucf.edu; swu@ucf.edu).

M.-C. Li, S.-L. Lee, and W.-C. Tsai are with the College of Optics and Photonics, University of Central Florida, Orlando, FL 32816 USA, and also with AU Optronics, Hsinchu 30078, Taiwan.

Color versions of one or more of the figures are available online at http://ieeexplore.ieee.org.

Digital Object Identifier 10.1109/JDT.2015.2408993

(QCBL) combined with a diffusing film (DF), as illustrated in Fig. 1. This structure was first proposed by Allied Signals about two decades ago [24]. In their design, the QCBL confines light to within $\pm 10^{\circ}$ (half-maximum) with respect to the normal direction, so that within LC layer the nearly-normal light experiences about the same phase retardation throughout the viewing cone. A diffusing screen is located above the LC layer, within which there is an array of 3-D tapered microstructures that transmits and redirects the light via total internal reflection (TIR). Since the microstructures are tapered toward the upper end, the propagation angle of beams with respect to normal direction gradually increases as they experience TIR on the lateral surfaces of the microstructures. With this diffusive film, the output brightness has a FWHM$\sim \pm 30^{\circ}$, which is a typical value for LCDs nowadays. What's more, the color shift and off-axis image distortion are greatly suppressed.

While this could theoretically be a universal solution for all kinds of LCDs, it faces following challenges. 1) The efficiency and uniformity of QCBL are usually not as good as those of conventional backlight. 2) A diffusive screen laminated on top of the LC panel can possibly cause glare and reduce the ambient contrast ratio, especially if it's based on a heavy diffuser. 3) The output brightness distribution is still limited to $\pm 30^{\circ}$, showing no significant improvement over other LCDs with simpler structures, and is much narrower than the Lambertian-like OLED emission.

In this review paper, we will discuss the previous QCBL and DF designs, and propose a novel design that giving LCD an OLED-like luminance distribution, while eliminating color shift and off-axis image distortion, and maintaining high contrast ratio at large viewing angles. Four popular LC modes are considered: twisted nematic (TN), vertical alignment (VA), in-plane switching (IPS) and fringing field switching (FFS). TN has been commonly used in notebook computers because of its low cost and high transmittance; VA has been widely used in TVs because of its unprecedented contrast ratio; and IPS and FFS have been widely used in smart phones and pads because of their robustness to resist external pressure, which is critical for touch panels.

II. Quasi-Collimated Backlight and Engineered Diffuser

When the first QCBL-LC-DF system was published by Allied Signals in 1995 [24], the structures of QCBL and DF were not explicitly illustrated. During the past two decades, there has been ongoing research on utilizing collimated backlight combined with front diffusers in different LC modes [25]–[28]. However, it has not been adopted in commercial LCDs yet, as far as we are concerned, because highly efficient directional backlight is difficult to fabricate, while traditional front diffusers blur the graphical image, wash out the color, and lower the contrast ratio.

Directional backlight finds many applications in LCD. It can be utilized for private view, stereoscopic, and multi-view displays [29]–[34]. It also helps enhance the screen brightness at normal viewing angle. For conventional LCDs, backlight does not have to be strictly collimated. It's more accurate to call it non-Lambertian backlight with a certain angular distribution confinement. Therefore, the collimation of a conventional

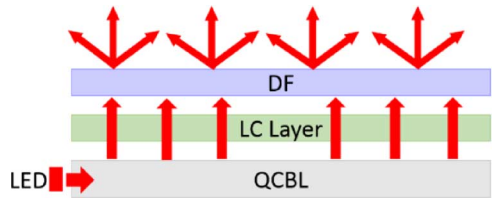

Fig. 1. Schematic diagram of the proposed LCD system comprised of a quasi-collimated backlight and a diffusing film.

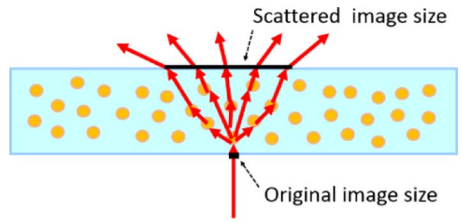

Fig. 2. Resolution degradation induced by top diffusing film.

backlight is done by simply using two crossed prism sheets, known as brightness enhancement films (BEFs), to confine the light in two directions [35], [36]. A two-dimensional micro-pyramid film was also developed to replace two BEFs in backlight modules [37]. More compact backlight unit consists of only a single-layer light guide plate (LGP) which integrates conventional LGP, BEFs, and diffusers [38]. There are also multi-layer micro-structured backlight plates as described in [39], in which the main layer serves to guide the light through, and a reflective layer with micro-structures on the bottom serves to collimate the backlight. Another multi-layer QCBL employs micro-lenses to obtain a fairly collimated backlight distribution [33], [40].

While all these directional backlight units have a relatively narrower light distribution than an ordinary LCD backlight, they are mostly designed to enhance the on-axis brightness, or for applications in 3D displays or other multi-view displays. Therefore, most luminance distributions are not really collimated, usually with FWHM over 30°. This is still too broad if we desire to totally eliminate color shift and image distortion under single-domain LCD scheme. In Section III, we will present a new QCBL whose light emission is confined in $\pm 7.5^{\circ}$ (FWHM), thus it is a very promising candidate for normal illumination of LCDs.

Now let's take a look at diffusing films. We divide DFs into three categories: scattering type, reflecting type, and refracting type. A typical scattering type diffuser adopts small particles dispersed or accumulated in a polymer film [28]. Although this type of diffusing film is rather easy to design and fabricate [28], [41]–[45], it is more likely to be used inside the backlight module rather than on top of LC cell toward the viewer's side. The major concern is that it hazes the image [44], resulting in degraded resolution and poor ambient contrast. Fig. 2 explains the reason. After transmitting through the scattering diffuser, what used to be a small image (say, a single pixel) is diffused into a larger size, thus crosstalk happens between neighboring pixels, resulting in a lower resolution. If one wants to achieve Lambertian light distribution, a heavy diffuser has to be applied, and the hazing problem would be very dramatic.

Reflecting type diffuser was used in the original QCBL-LC-DF structure proposed by Allied Signals [24], as pointed out in Section I. Recently, Sharp demonstrated a reflecting type DF with tapered micro-cavities fabricated by roll-to-roll process [46], [47]. To reduce ambient reflection, they applied a black matrix on top of the diffuser that covers the area where lights are not extracted from LCs, so that the ambient contrast ratio is increased. However, this tapered micro-cavity structure fails to bring in much improvement on the viewing angle of LCD, except at 270° azimuthal viewing direction, where the contrast ratio is increased from less than 10 to between 10 and 100, which is due to the necessary compromise between diffusing power, fabrication complexity, and energy transmittance. What's more, it doesn't show any evidence for improving the off-angle brightness of the screen.

Refraction type diffusers always come in the shape of thin films with surface-relief microstructures, such as micro-lens array, micro-spheres or micro-grooves [48]–[50], and are usually part of the backlight system rather than being placed on top of LC layer (viewer's side). Some specialized engineered diffusers [51]–[54] not only serve to broaden the viewing angle and improve the color mixing, but also create special luminance patterns and make the viewing direction controllable, as is in free-form optics. As the micro-optics fabrication technology keeps advancing [55], [56], structures with micrometer size can now be fabricated on thin glass or polymer substrates, which enables a variety of new applications in LCDs. Generally speaking, this kind of diffusers offer more design freedom and are more versatile. However they haven't been widely investigated and used in LCDs as top diffusers because of the ambient reflection induced glaring. Our following discussion about diffusers will focus on suppressing this problem.

A. Quasi-Collimated Backlight (QCBL)

Now let's take a look at our design of quasi-collimated backlight.

As illustrated in Fig. 3, the QCBL consists of two micro-structured glass light guide layers, labeled A and B, and a reflector at the bottom. Layers A and B can be laminated together with a low refractive index glue (e.g. NOA 1315), which creates an index mismatch for TIR. Instead of laminating two layers, one can also choose to simply leave a thin air gap between them to create an interface to allow for TIR. Edge-lit LED beams are coupled into layer A, and experience multiple TIRs as they travel along the light guide until hitting one of the small pyramid shaped hollows at the bottom of layer A, where beams are deflected dramatically and enter layer B. The focal points of the micro-lens array on layer B overlap with the hollows in layer A, so that the lens receives incident light as if it were emitted from its focus, and collimates the output light. In our design, the thickness of layer A and layer B is 0.5 mm each. The side length of hollows is 250 μm, and the radius of the micro-lens is 600 μm. Shrinking or enlarging the QCBL in proportion does not change the angular distribution of the output, as long as the size of the micro-structures is significantly larger than the visible wavelengths. We achieved over 70% efficiency, and the FWHM of the emission is 15°, as in Fig. 3. Note that in Fig. 3(c), at $\pm 10°$

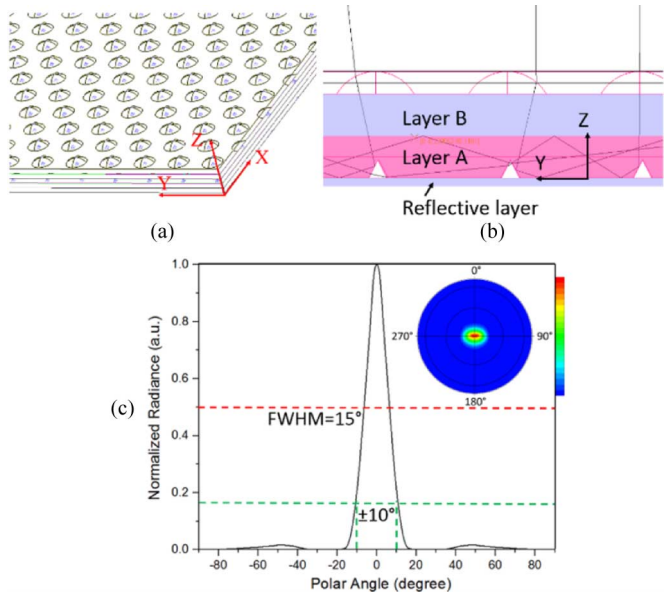

Fig. 3. Schematic diagram of QCBL: (a) 3D schematic diagram of the LGP; (b) cross section of the LGP; and (c) luminance versus viewing angle.

the radiance is only 17% of the maximum value. We'll use this in latter discussions.

When it comes to luminance uniformity, two structures are considered. The difference between two structures are the placement of the microstructures on layer A and layer B. Shown in Fig. 4, one structure has hexagonal aligned micro-lenses and hollows with edge-lit backlight at both ends of the backlight plate, whose uniformity is >91%. The other is a conventional edge-lit LGP with squarely placed lens and hollow array with uniformity >85%. In the hexagonal placed structure, micro-lenses and hollows have a uniform spatial density, while in the squarely placed structure, lens and hollow array is more condensed at the far end of the LGP with respect to the position of the LED light source. Comparing these two structures, some may prefer the hexagonal one for the better uniformity, while others may favor conventional single-side-lit using squarely aligned lens array. To yield yet better uniformity, randomization can be introduced, and it's favorable to have the micro-lenses and -grooves smaller, if it's achievable in fabrication.

B. Diffusing Film

The engineered diffusing film (EDF) serves to broaden the viewing angle and reduce the color shift at oblique viewing direction. Fig. 5 depicts the EDF structure. It consists of a thin film and a hexagonal array of transparent ellipsoid-like micro-structures, which diffract incident beams to the desirable direction. To suppress ambient reflection, the top surface of the EDF is coated with an absorptive layer with transparent pupils as the output region. Fig. 5(a) is the top view of the EDF. The yellow area represents black matrix which absorbs light, while the purple circles correspond to transparent pupils that are aligned with the microstructures. Since the backlight is quite collimated, the microstructures on the EDF serve to focus beams to the positions of transparent pupils, rendering a rather high transmittance. An example of ray tracing is shown in Fig. 5(b). The micro-structures at the bottom of EDF can be

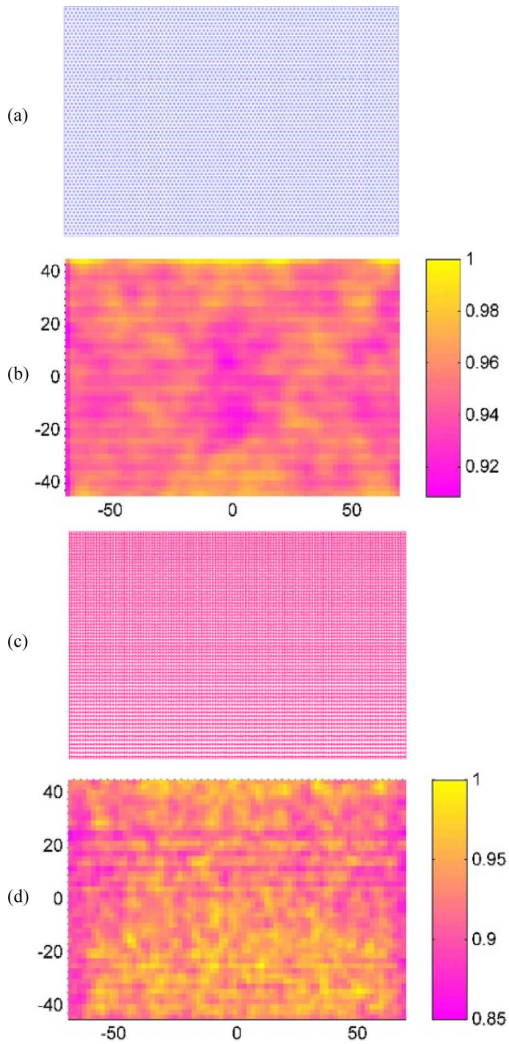

Fig. 4. Two schemes of backlight plate. (a) Hexagonal micro- structured array and (b) its brightness spatial uniformity. (c) Square micro-structured array and (d) its brightness spatial uniformity.

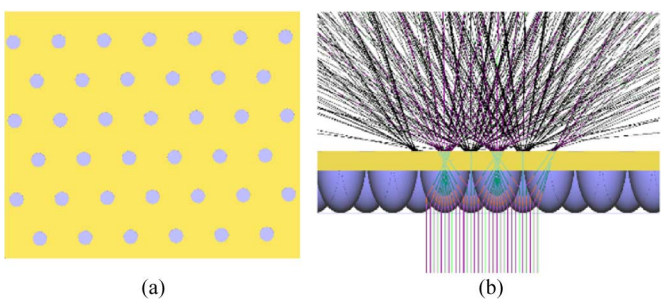

Fig. 5. Structure engineered diffusing film: (a) Top view, and (b) Side view with ray tracing.

designed using free-form optics methods to specifically convert the luminance distribution of the output of the above mentioned QCBL to what is desired. The principle of the free-form design is based on conservation of energy and ray tracing, as Fig. 6 shows. Fig. 6(a) is a single free-form microstructure. Assume the backlight is perfectly collimated, and the free-form micro-structure has rotational symmetry along z-axis. P(r,Z) is

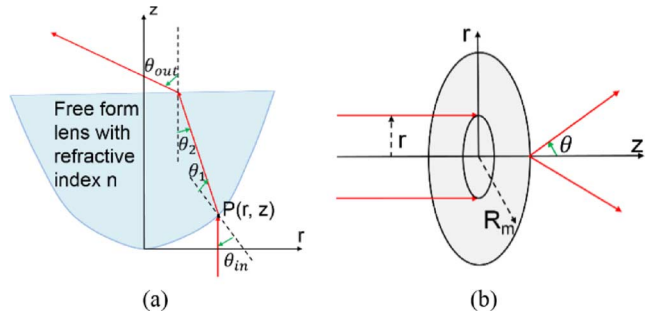

Fig. 6. Design principles of the engineered diffuser: (a) Ray tracing, and (b) Energy conservative mapping.

a point on the free-form surface where light is incident on. The incident and emergent angles on the free-form surface are $\theta_{\rm in}$ and θ_1, respectively, while the incident and emergent angles on the plat top surface are θ_2 and $\theta_{\rm out}$, respectively. Beams incident on the EDF experience two diffractions: the first one upon the freeform surface, and the second one on the output plat surface. According to geometrical optical ray tracing, the relation between $\theta_{\rm in}$ and $\theta_{\rm out}$ can be expressed as

$$\sin(\theta_{\rm out}) = n - \sin\left\{\arcsin\left[\frac{\sin(\theta_{\rm in})}{n}\right] - \theta_{\rm in}\right\} \qquad (1)$$

where n is the refractive index of the material. The slope of the free-form surface at point $P(r, Z)$ is associated with $\theta_{\rm in}$ by

$$\frac{dz}{dr} = -\tan(\theta_{\rm in}). \qquad (2)$$

Fig. 6(b) shows transform of collimated light into a desired light distribution. The grey circle is the projection of the free-form shape along its axis, while R_m is its maximum radius. Light incident on the area within radius r is refracted to a cone whose maximum polar angle is θ. That's to say, beams incident on the ring $r \sim r + \Delta r$ are refracted to a cone between θ and $\theta + \Delta\theta$. Let us say the targeted intensity distribution is $I = I_0 \cos^a(\theta_{\rm out})$, where I (W/sr) is the final intensity distribution after light passing through the EDF, and I_0 and a are constants. When $a = 1$, the intensity distribution is Lambertian. Other distribution can be approximated by adjusting the value of a. If the incident collimated light has a uniform illuminance E (W/m^2), according to energy conservation, I_0 and E are related by

$$\pi R_m^2 E = 2\pi \int_0^{\frac{\pi}{2}} I(\theta) sin(\theta) d\theta. \qquad (3)$$

The above equation solves I_0 with respect to E

$$I_0 = (\mathrm{a}+1) R_m^2 \mathrm{E}/2. \qquad (4)$$

To achieve a desirable $I(\theta_{\rm out})$, a mapping between the incident position $P(r, Z)$ and the emergence angle $\theta_{\rm out}$ needs to be established, which is also based on energy conservation

$$\pi \mathrm{r}^2 E = 2\pi \int_0^{\theta_{\rm out}} I(\theta) sin(\theta) d\theta. \qquad (5)$$

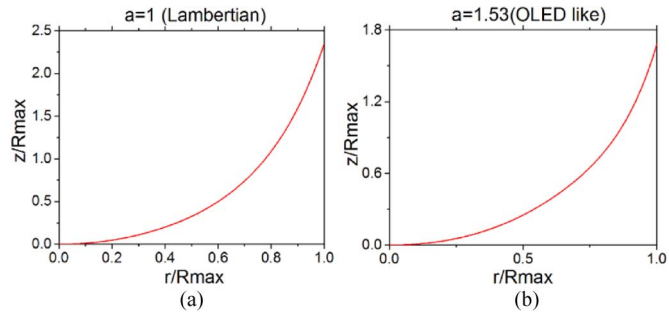

Fig. 7. Profiles of freeform microstructures on EDF: (a) Lambertian light distribution, and (b) OLED-like light distribution.

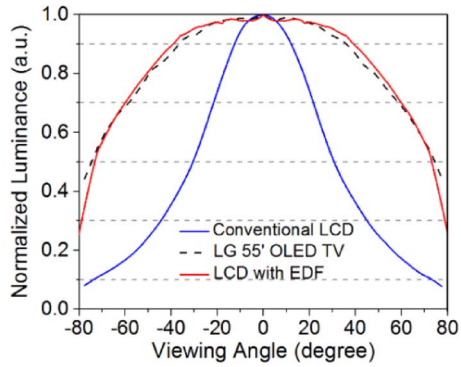

Fig. 8. Normalized luminance distribution of conventional LCD, LG's 55-inch OLED, and our proposed LCD with EDF.

Combining (4) and (5), r can be solved with respect to θ_{out}

$$r^2 = R_m^2 \left(1 - cos^{a+1}(\theta_{\text{out}})\right). \tag{6}$$

In summary, the following three relations jointly define the free-form surface shape: geometrical optics ray tracing relation [see (1)], slope-position relation [see (2)], and energy conservative mapping [see (6)].

After pre-designing the free-form shape, one needs to further consider the Fresnel reflection on each surface, and also optimize the EDF based on the real incident luminance distribution, which is hardly perfectly collimated. Both of them can be done by iterations with the predefined shape as initial condition. We calculated point-by-point the freeform outline of the microstructure when the desired final luminance distribution is Lambertian or OLED-like, and the final profiles of free-form surfaces in these two cases are shown in Fig. 7. The micro-structure profile in Fig. 7(a) is designed for Lambertian luminance distribution, and the profile in Fig. 7(b) is designed to achieve the light distribution of LG's 55-inch OLED TV [3]. We found that for this OLED display, the value of a is 1.53, and the ray tracing shown in Fig. 5(b) uses the profile in Fig. 7(b) with normal incident beams. The diffusing power of this EDF is very strong, and since the refraction on the surface is deterministic, this structure won't reduce the resolution of the displays.

In conventional freeform design for illumination applications, superellipse is a quite common function to fit the freeform profile. However in our design, we found that superellipse is not an accurate approximation, with normalized standard deviation $\sigma = 0.0154$ and 0.0064 for freeform profiles designed for Lambertian luminance and OLED-like luminance, respectively. Therefore, we tried to use polynomial to fit the curves in Fig. 7. The fitting function for both curves is

$$z = A_2 r^2 + A_4 r^4 + A_6 r^6 + A_8 r^8 \tag{7}$$

There is no odd term or constant term since the profile is symmetric and at r = 0 we define the height z to be zero. The fitting parameters $[A_2, A_4, A_6, A_8]$ for the two curves in Fig. 7(a) and Fig. 7(b) are $[1.1765, 0.3578, 0.5361, 0.2807, 0.0015]$ and $[0.8186, 1.0784, -1.6707, 1.4535, 0.0033]$, respectively.

Next, let us combine QCBL and EDF, and compare their performance with conventional LCD and OLED systems. Fig. 8 shows the angular dependent luminance in conventional LCD, LG's 55-inch OLED TV, and our QCBL-LC-EDF display system using the EDF microstructures shown in Fig. 7(b). The luminance and viewing angle relation of our system resembles that of the OLED TV very well. In comparison, one may argue that the luminance in current LCD backlight modules, a brightness enhancement film (BFE) [57] is layered above the diffuser to enhance the normal view brightness, so that the viewing angle is deliberately narrowed. However, even without the BEF, the luminance distribution of conventional edge-lit backlight is Gaussian-like with FWHM usually limited within $\pm 50^\circ$ [58], [59], while our structure broadens the FWHM to $\pm 75^\circ$ as Fig. 8 shows. Moreover, one should take into consideration not only the luminance distribution, but also the image quality at large viewing angle. If the light is already diffused enough before reaching the LC layer, varied light paths would result in varied transmittance, hence deteriorating the color performance and grey level accuracy. Our design, however, can maintain exceptional image quality at large viewing angle, which will be discussed in Section IV. The transmittance of the EDF resulting in OLED-like luminance distribution is about 65%. Thanks to the absorptive area that covers over 80% of the output surface [Fig. 5(a)], the ambient reflection is only 3%, which ensures superior image quality under direct sunlight or other strong ambient light. Note that the absorptive area hardly affects the transmission efficiency of the EDF. From Fig. 5(b), we can see the freeform microstructures focusing beams onto the pupil, so that most light coming from the display gets transmitted.

To further examine the diffusing effectiveness of the EDF, let us define a function $M(\theta_{\text{out}}, \varphi_{\text{out}}, \theta_{\text{in}}, \varphi_{\text{in}})$ to represent the mapping correspondence of the incident angle and the emerging angle. As pictured in Fig. 9(a), θ_{in} and φ_{in} stand for the polar and azimuthal angles of the incident beam measured from the normal of the EDF surface, while θ_{out} and φ_{in} represent the angles of the emerging beam. We scan θ_{in} and φ_{in} of the incident light with fixed incident luminance I_0, and record the output luminance distribution $I(\theta_{\text{out}}, \varphi_{\text{out}})$ on a far field receiver. The intensity distribution is then normalized and saved in the 4D matrix $M(\theta_{\text{out}}, \varphi_{\text{out}}, \theta_{\text{in}}, \varphi_{\text{in}})$ as

$$M(\theta_{\text{out}}, \varphi_{\text{out}}, \theta_{\text{in}}, \varphi_{\text{in}}) = \frac{I_{receiver}(\theta_{\text{out}}, \varphi_{\text{out}}; \theta_{\text{in}}, \varphi_{\text{in}})}{I_0}. \tag{8}$$

That is to say, $M(\theta_{\text{out}}, \varphi_{\text{out}}, \theta_{\text{in}}, \varphi_{\text{in}})$ indicates how rays incident on the EDF at angle $(\theta_{\text{in}}, \varphi_{\text{in}})$ contribute to rays emerging from the EDF at angle $(\theta_{\text{out}}, \varphi_{\text{out}})$. Fig. 9(b) gives

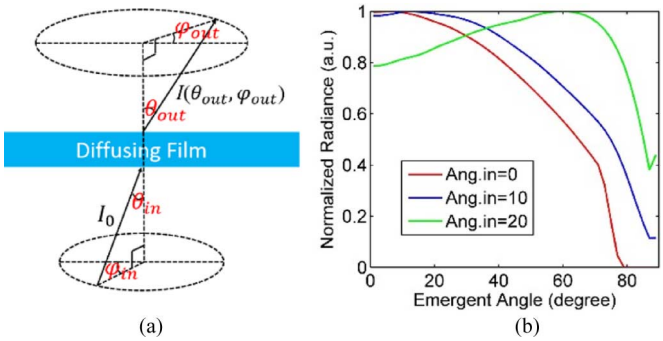

Fig. 9. (a) EDF mapping examination scheme, and (b) EDF mapping examination results.

three lines as examples. The red one illustrates the integration $\int\int_{0^\circ}^{360^\circ} M(\theta_{\rm in}=0^\circ,\varphi_{\rm in},\theta_{\rm out},\varphi_{\rm out})d\varphi_{\rm in}d\varphi_{\rm out}$ versus $\theta_{\rm out}$, and the blue and green lines plot the same integration when $\theta_{\rm in}$ is 10° and 20°, respectively. It's apparent that the output angular distributions are very close to each other when the incident light is tilted up to 10°. From Fig. 3(c), we know that the backlight is mostly confined in ±10°, so it's safe to say that this EDF works pretty well with the proposed QCBL. Another thing to be noticed is that for perfectly normal incident beams, output light radiance decays to zero when the viewing angle is over 80° [red curve in Fig. 9(b)]. This is compensated by slightly oblique beams incident on the EDF from, say 10°, which gives sufficient output at large viewing angle, but still maintains good LC performances.

III. LCD System Characterization

To analyze how well the whole LCD system works, let us define the following system transmission:

$$T_{\rm sys}(\theta_{\rm out},\varphi_{\rm out},V)=\int_0^{2\pi}\int_0^{\frac{\pi}{2}} M(\theta_{\rm out},\varphi_{\rm out},\theta_{\rm in},\varphi_{\rm in})I_s(\theta_{\rm in},\varphi_{\rm in}) \cdot T_{LC}(\theta_{\rm in},\varphi_{\rm in},V,550\ {\rm nm})d\varphi_{\rm in}d\theta_{\rm in} \tag{9}$$

where $I_s(\theta_{\rm in},\varphi_{\rm in})$ is the normalized angular intensity distribution of the QCBL emission in Section II-A (refer to Fig. 3(c)), $T_{LC}(\theta_{\rm in},\varphi_{\rm in},V,\lambda=550\ {\rm nm})$ the LC panel transmittance when the voltage V is applied, and $M(\theta_{\rm out},\varphi_{\rm out},\theta_{\rm in},\varphi_{\rm in})$ the mapping function defined in Section II-B.

The contrast ratio (CR) is defined as

$$CR(\theta_{\rm out},\varphi_{\rm out})=\frac{T_{sys}(\theta_{\rm out},\varphi_{\rm out},V_{on})}{T_{sys}(\theta_{\rm out},\varphi_{\rm out},V_{\rm off})}. \tag{10}$$

To compare our design with conventional LCD products without directional backlight below LC panel or diffusing film above LC penal, we further define the transmission of conventional LCD system as

$$T_{\rm con}(\theta,\varphi,V)=I_{con}(\theta,\varphi)\cdot T_{LC}(\theta,\varphi,V,\lambda=550\ {\rm nm}) \tag{11}$$

where $I_{\rm con}(\theta,\varphi)$ is the normalized emission from conventional LCD backlight unit (BLU). Note that the diffusing layer in conventional LCD is buried inside the BLU, so the propagating direction does not change once light has exited the BLU. Therefore, integrating (8) is not necessary, and $\theta_{\rm out}=\theta_{\rm in}=\theta$, $\varphi_{\rm out}\varphi_{\rm in}=\varphi$. The CR is thus simply the ratio of LC transmittance in the voltage-on and -off states

$$\begin{aligned} CR(\theta,\varphi)&=\frac{T_{con}(\theta,\varphi,V_{on})}{T_{con}(\theta,\varphi,V_{\rm off})}\\ &=\frac{I_{con}(\theta,\varphi)\cdot T_{LC}(\theta,\varphi,V_{on},\lambda=550\ {\rm nm})}{I_{con}(\theta,\varphi)\cdot T_{LC}(\theta,\varphi,V_{\rm off},\lambda=550\ {\rm nm})}\\ &=\frac{T_{LC}(\theta,\varphi,V_{on},\lambda=550\ {\rm nm})}{T_{LC}(\theta,\varphi,V_{\rm off},\lambda=550\ {\rm nm})}. \end{aligned} \tag{12}$$

IV. LCD Performances With QCBL and EDF

We simulated the LCD system performances with our proposed QCBL and EDF. Four commonly employed LC modes are investigated: single-domain TN, VA, IPS, and FFS (using both positive and negative $\Delta\varepsilon$ LC materials). In our simulation, we did not take into account the pixel structures or black matrix in the LCD system, however the analysis is universal for any conventional RGB pixel schemes. We find that our designs exhibit outstanding performances in all modes.

A. TN LCD

Conventional TN LCD [60] exhibits a narrow and asymmetric viewing cone because the LC directors are tilted up under applied voltage so that the incident light experiences different effective birefringence when viewed from different oblique angles. The viewing angle of a TN LCD without any compensation is very narrow. At 40° viewing angle, the CR already drops to about 10. To achieve wider viewing angle, a variety of compensation films have been developed, among which wide-view (WV) film developed by Fuji Photo [13] is of great value and acknowledgement. WV film is made of a discotic material with specifically designed hybrid alignment to compensate for birefringence induced by TN in dark state. With the help of WV film, the viewing cone with CR over 10:1 exceeds 80°, however the viewing cone for CR larger than 300 is still very narrow, so further improvement is in need to boost the contrast ratio. In Fig. 10(a), we illustrate the CR of TN-LC (Merck MLC-6686, $\Delta n=0.097$, $\Delta\varepsilon=10$, cell gap 5 μm) enhanced by QCBL, EDF and WV film, with a CR of 1000:1 even at 85° viewing cone, which is the best result ever been achieved. The reason that QCBL combined with EDF can yield such excellent result is that the light incident on the TN cell is mostly confined in ±10°, within which the CR of the TN cell itself is very high. In Section II-B, we proved that the EDF serves to spread out incident light, and even those beams emitting from EDF with a polar angle as large as 85° are quite collimated, i.e., within the ±10° cone, when passing through the LC layer. Thus, high contrast ratio at large oblique angle can be achieved.

We also calculated the gamma curve of the TN-LCD with QCBL and EDF. The simulation results are presented in Fig. 10(b). Conventional TN-LCD suffers from serious gray level inversion at large viewing angles, but our design gives almost overlapping curves for 0°, 20°, 40°, and 60° viewing angles. To quantitatively characterize the off-axis image quality, an off-axis image distortion index D defined in [5] is used. If

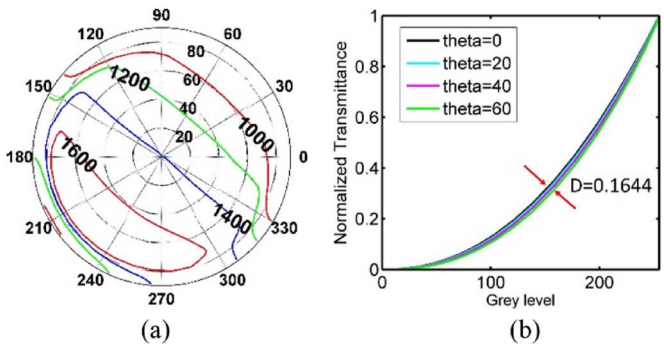

Fig. 10. Simulated (a) isocontrast contour and (b) gamma curve of a single-domain TN LCD with QCBL, EDF, and WV film.

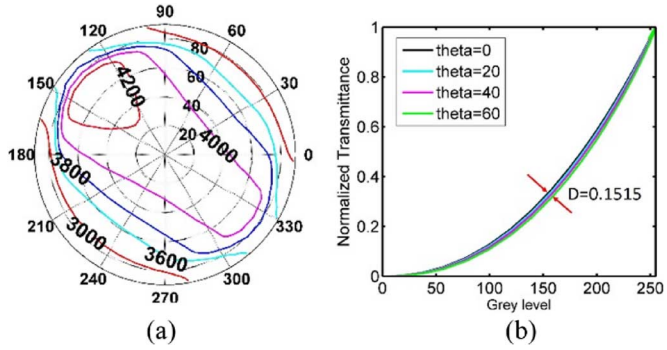

Fig. 11. (a) Simulated isocontrast contour of a single-domain VA LCD with QCBL, EDF, and compensation films. (b) Simulated gamma curves at the specified theta angles.

D < 0.2, then the image distortion is indistinguishable by the human eye. As shown in Fig. 10(b), D is only 0.1644. Such a small D implies that the color shift is almost negligible, even for a single-domain TN-LCD.

B. VA LCD

Viewing angle is an important issue for VA LCD [61], which has been widely used in TVs because of its high contrast ratio. A single-domain VA has very narrow viewing angle. To widen viewing angle, a common approach is to use multi-domain vertical alignment (MVA) structure. However MVA requires at least four domains to show wide-view characteristics, which not only increases manufacturing difficulties but also decreases transmittance and induces disclination lines. It would be highly desirable if one can get wide view like MVA but with a single domain structure. Here, we analyze the performance of our design under the single-domain VA configuration in a manner similar to that in Section IV-A, and the results are quite exciting. In our simulation, Merck MLC-6882 ($\Delta n = 0.097$ and $\Delta\varepsilon = -3.1$) is used as the host material, and the cell gap is 4 μm.

Fig. 11(a) depicts the isocontrast contour of a single-domain VA LCD sandwiched between the proposed QCBL and the EDF, with a negative-C and a positive-A compensation films. These two films can be replaced by a biaxial film. From Fig. 11(a), the maximum contrast ratio exceeds 4200:1, while keeping above 3000:1 within the 80° viewing cone. The maximum CR is off-center because for single domain VA, the minimum phase retardation in dark state is actually not along normal viewing direction, since there is no multi-domain structure to compensate for the phase retardation induced by pretilt angle (in our simulation, the pretilt angle is 2° along 135° azimuthal direction). After the viewing angle being broadened by the EDF, the isocontrast contours are also broadened, so that in Fig. 11(a) the maximum contrast occurs at around 60° in 135° azimuthal direction.

We also simulated the gamma curve and results are plotted in Fig. 11(b). Conventional single-domain VA LCD, if not compensated, suffers from serious grayscale inversion at large viewing angles. But again, our design gives almost overlapping gamma curves from 0° to 60° viewing angles. The off-axis image distortion index D is 0.1515.

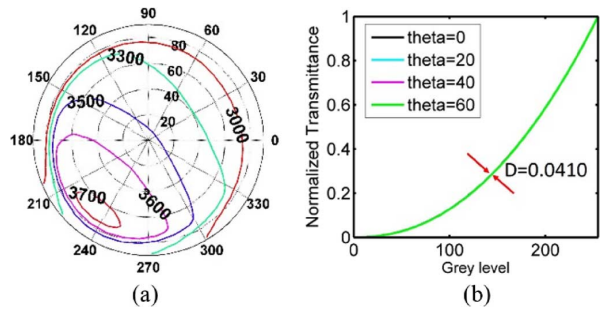

Fig. 12. Simulated (a) isocontrast contours and (b) gamma curves of the single-domain IPS LCD with QCBL and EDF. No compensation film is applied.

C. IPS LCD

Similar analysis can be applied to IPS LCD [62] as well, which is a dominant technology for mobile phones and tablets. Fig. 12(a) shows the simulated isocontrast contours of our proposed QCBL-IPS-EDF system. We used MLC-6686 in the simulation, and the cell gap is 3.86 μm, rubbing angle is 80°, pretilt angle is 2°, and electrode width and gap are 5 μm both. Note that in this LC mode, no compensation film is employed, so the maximum CR is not as high as that of above-mentioned VA mode. However, the 3000:1 contour covers the entire 70° viewing cone. More amazingly, the off-axis image distortion index D is as small as 0.0410. The four gamma curves plotted in Fig. 12(b) can hardly be distinguished.

D. FFS LCD

For fringe field switching mode, both positive $\Delta\varepsilon$ LC (p-FFS) and negative $\Delta\varepsilon$ LC (p-FFS) have been used in smart phones and pads. According to [63]–[66], n-FFS exhibits advantages over p-FFS in higher transmittance, less cell gap sensitivity, and single gamma curve. In our simulations, we used MLC-6686 for p-FFS (cell gap 3.87 μm, rubbing angle 80°, pretilt angle 2°, electrode width 2 μm, electrode gap 3 μm) and UCF-N1 ($\Delta n = 0.116$, $\Delta\varepsilon = -3.82$) for n-FFS (cell gap 3.02 μm, rubbing angle 10°, pretilt angle 2°, electrode width 2 μm, electrode gap 3 μm). Fig. 13 shows the system performance of single-domain n-FFS and p-FFS with the proposed QCBL and EDF. Not only the contrast ratio is larger than 3000:1 even when the viewing angle is 80°, gamma curves also overlap quite well. The reason for such a high contrast ratio is mainly due to the increased transmittance at bright state: in FFS mode with narrow

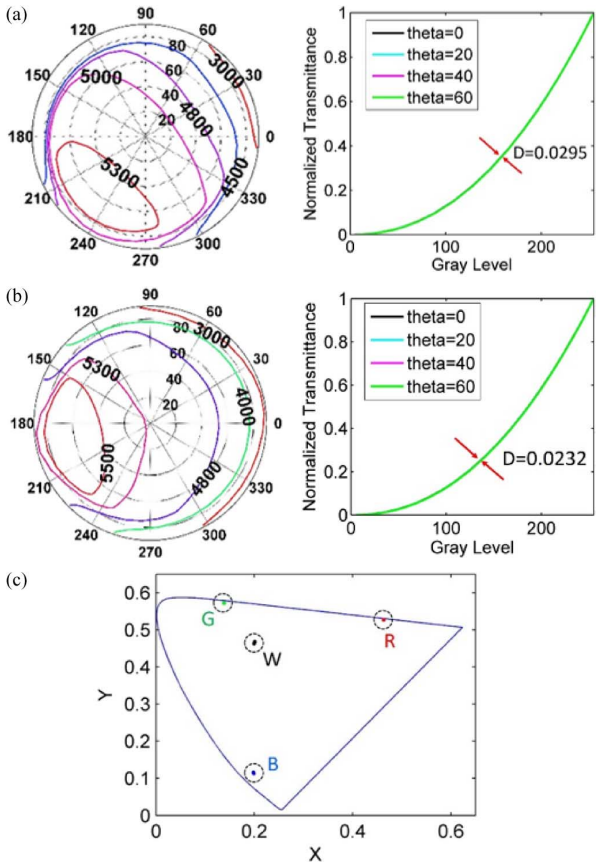

Fig. 13. Simulated isocontrast contours and gamma curves of (a) n-FFS and (b) p-FFS with QCBL and EDF, and (c) color shift of p-FFS at 60° viewing angle in CIE 1976 diagram.

electrode width and gap, the electric field can easily penetrate through the LC layer, so that the phase retardation is more uniform in lateral direction than in IPS cells. The image distortion is D=0.0295 for p-FFS and D=0.0232 for n-FFS. What's more, Fig. 13(c) shows the color shift of p-FFS at 60° in CIE1976 diagram. The white point color shift value $\Delta u'v'$ is as small as 0.003, which is much smaller than 1 JNCD (Just Noticeable Color Difference, $\Delta \mathrm{u'v'} = 0.02$). This is so far the best LCD in terms of contrast ratio, image distortion, and color shift, as far as we are concerned. More importantly, no compensation film is used in this structure, so that the LCD system can be very thin and simple.

V. Conclusion and Future Outlook

We proposed a quasi-collimated backlight whose FWHM is only 15°, with good transmittance and good spatial uniformity, and also demonstrated an engineered diffuser with free-form optical design. The combination of QCBL and EDF can be universally used for all major LC modes, and gives each of these modes very high contrast ratio and extremely wide viewing angle. Moreover, the absorptive layer on the output surface of the EDF reduces the ambient reflection to 3%, and keeps a good resolution of the display.

The designs of directional backlight and top engineered diffuser are still evolving, and emphases can be put on the following aspects: 1) further increasing the spatial uniformity and efficiency of the backlight; 2) optimize the design of the engineered diffuser to achieve higher transmittance and more versatile diffusing power; and 3) preferably make diffuser somewhat switchable, so that LCDs can be switched between privacy mode and multi-viewer mode. Despite these technical challenges, the combination of quasi-collimated backlight with engineered diffuser proves to enhance the display quality very effectively. The developments of directional backlights and diffusers are pushing LCD industry to the next level, and color shift free, ultra wide view LCDs are just around the corner.

Acknowledgment

The authors are indebted to H. Chen, F. Peng, J. Yuan, and D. Xu for valuable discussion.

References

[1] D. Barnes, "5.1: Invited paper: LCD or OLED: Who wins?," in *SID Symp. Dig. Tech. Papers*, 2013, vol. 44, no. 1, pp. 26–27.
[2] Z. Luo, D. Xu, and S.-T. Wu, "Emerging quantum-dots-enhanced LCDs," *J. Display Technol.*, vol. 10, no. 7, pp. 526–539, Jul. 2014.
[3] J. K. Yoon *et al.*, "27.2: The study of picture quality of OLED TV with WRGB OLEDs structure.," in *SID Symp. Dig. Tech. Papers*, 2013, vol. 44, no. 1, pp. 326–329.
[4] R. M. Soneira, "iPhone 6 Display Technology Shoot-Out," [Online]. Available: http://www.displaymate.com/iPhone6_ShootOut.htm Accessed on: Mar. 11, 2015
[5] S. S. Kim, B. H. Berkeley, K. H. Kim, and J. K. Song, "New technologies for advanced LCD-TV performance," *J. Soc. Inf. Display*, vol. 12, no. 4, pp. 353–359, 2004.
[6] S.-H. Ji, S. H. Lee, and G.-D. Lee, "Optimization of an optical configuration in a vertical alignment liquid crystal cell for wide viewing angle," *Appl. Opt.*, vol. 48, no. 1, pp. 48–54, 2009.
[7] Q. Hong, T. X. Wu, X. Zhu, R. Lu, and S.-T. Wu, "Extraordinarily high-contrast and wide-view liquid-crystal displays," *Appl. Phys. Lett.*, vol. 86, no. 12, p. 121107, 2005, Art ID 121107.
[8] M. Jiao, Z. Ge, and S.-T. Wu, "Wide-view MVA-LCDs with an achromatic dark state," *J. Display Technol.*, vol. 5, no. 5, pp. 141–146, May 2009.
[9] M. Jiao, Z. Ge, and S.-T. Wu, "Broadband wide-view LCDs with small color shift," *J. Display Technol.*, vol. 5, no. 8, pp. 331–334, Aug. 2009.
[10] M. Jiao, S. Gauza, Y. Li, J. Yan, S.-T. Wu, and T. Chiba, "Negative A-plates for broadband wide-view liquid crystal displays," *Appl. Phys. Lett.*, vol. 94, no. 10, 2009, Art ID 101107.
[11] X. Zhu, Z. Ge, and S.-T. Wu, "Analytical solutions for uniaxial-film-compensated wide-view liquid crystal displays," *J. Display Technol.*, vol. 2, no. 1, pp. 2–20, Mar. 2006.
[12] H. Mori *et al.*, "32.3: Novel optical compensation method based upon a discotic optical compensation film for wide-viewing-angle LCDs.," in *SID Symp. Dig. Tech. Papers*, 2003, vol. 34, no. 1, pp. 1058–1061.
[13] H. Mori, Y. Itoh, Y. Nishiura, T. Nakamura, and S. Shinagawa *et al.*, "Performance of a novel optical compensation film based on negative birefringence of discotic compound for wide-viewing-angle twisted-nematic liquid-crystal displays," *Jpn. J. Appl. Phys.*, vol. 36, no. 1R, pp. 143–147, 1997.
[14] H. Mori, "The wide view (WV) film for enhancing the field of view of LCDs," *J. Display Technol.*, vol. 1, no. 2, pp. 179–186, 2005.
[15] J. Chen, K. H. Kim, J. J. Jyu, J. H. Souk, J. R. Kelly, and P. J. Bos, "21.2: Optimum film compensation modes for TN and VA LCDs.," in *SID Symp. Dig. Tech. Papers*, 1998, vol. 29, no. 1, pp. 315–318.
[16] Y. Liu, Y.-F. Lan, Q. Hong, and S.-T. Wu, "Compensation film designs for high contrast wide-view blue phase liquid crystal displays," *J. Display Technol.*, vol. 10, no. 1, pp. 3–4, 2014.
[17] S. Nishida, T. Suzuki, and M. Suzuki, "In-plane switching type liquid crystal display having a compensation layer with the principal optical axis extending perpendicularly to the substrate," U.S. Patent 6 115 095, Sep. 5, 2000.
[18] M. Schadt, H. Seiberle, and A. Schuster, "Optical patterning of multi-domain liquid-crystal," *Nature*, vol. 381, pp. 212–215, 1996.
[19] R. A. John and S.-C. A. Lien, "Liquid crystal displays having multi-domain cells," U.S. Patent 5 309 264, May 3, 1994.
[20] S. W. Park *et al.*, "Multi-domain vertical alignment liquid crystal displays with ink-jet printed protrusions," *Liq. Cryst.*, vol. 39, no. 4, pp. 501–507, 2012.

[21] K.-H. Kim *et al.*, "Pixel electrode structure for high transmittance in a multi-domain vertical alignment liquid crystal display device," *J. Phys. D Appl. Phys.*, vol. 45, no. 6, 2012, Art ID 065103.
[22] K.-H. Kim *et al.*, "High-transmittance multi-domain vertical alignment liquid crystal device with protrusion structure," *J. Opt. Soc. Kor.*, vol. 16, no. 2, pp. 166–169, 2012.
[23] J. Ma *et al.*, "Analysis of display defects in the multi-domain vertical alignment mode liquid crystal display," *Displays*, vol. 33, no. 4, pp. 186–190, 2012.
[24] S. Zimmerman *et al.*, "Viewing-angle-enhancement system for LCDs," *J. Soc. Inf. Display*, vol. 3, no. 4, pp. 173–176, 1995.
[25] K. Käläntär, "A directional backlight with narrow angular luminance distribution for widening the viewing angle for an LCD with a front-surface light-scattering film," *J. Soc. Inf. Display*, vol. 20, no. 3, pp. 133–142, 2012.
[26] A. Tagaya and Y. Koike, "55.1: Invited paper: A novel LCD structure using transparent polymers free of birefringence and scattering polymers free of wavelength dependency.," in *SID Symp. Dig. Tech. Papers*, 2012, pp. 737–740.
[27] H. Takemoto *et al.*, "The performance of collimated backlight and front diffusing systems on several LC modes," in *Proc. IDW'09*, 2009, pp. 1907–1908.
[28] T. Saruta, A. Tagaya, and Y. Koike, "A wide-viewing-angle liquid-crystal display using front-scattering film and directional backlight.," *SPIE OPTO. Int. Soc. Opt. Pho.*, pp. 79550G–79550G-9, 2011.
[29] A. Travis *et al.*, "Collimated light from a waveguide for a display backlight," *Opt. Express*, vol. 17, no. 22, pp. 19714–19719, 2009.
[30] T. Sasagawa *et al.*, "P-51: Dual directional backlight for stereoscopic LCD.," in *SID Symp. Dig. Tech. Papers*, 2003, vol. 34, no. 1, pp. 399–401.
[31] D. Fattal *et al.*, "A multi-directional backlight for a wide-angle, glasses-free three-dimensional display," *Nature*, vol. 495, no. 7441, pp. 348–351, 2013.
[32] K.-W. Chien and H.-P. D. Shieh, "Time-multiplexed three-dimensional displays based on directional backlights with fast-switching liquid-crystal displays," *Appl. Opt.*, vol. 45, no. 13, pp. 3106–3110, 2006.
[33] T.-C. Teng and J.-C. Ke, "A novel optical film to provide a highly collimated planar light source," *Opt. Express*, vol. 21, no. 18, pp. 21444–21455, 2013.
[34] C.-H. Chen, Y.-C. Yeh, and H.-P. D. Shieh, "3-D mobile display based on Moiré-free dual directional backlight and driving scheme for image crosstalk reduction," *J. Display Technol.*, vol. 4, no. 1, pp. 92–96, 2008.
[35] S. Kobayashi, S. Mikoshiba, and S. Lim, *LCD Backlights*. Chichester, U.K.: Wiley, 2009.
[36] M. Suzuki, "Two approaches to the luminance enhancement of backlighting units for LCDs," *J. Soc. Inf. Display*, vol. 7, no. 3, pp. 157–161, 1999.
[37] L. Lin, T. Shia, and C. Chiu, "Silicon-processed plastic micropyramids for brightness enhancement applications," *J. Micromech. Microeng.*, vol. 10, no. 3, pp. 395–400, 2000.
[38] J.-H. Lee, H.-S. Lee, and B.-K. Lee *et al.*, "Simple liquid crystal display backlight unit comprising only a single-sheet micropatterned polydimethylsiloxane (PDMS) light-guide plate," *Opt. Lett.*, vol. 32, no. 18, pp. 2665–2667, 2007.
[39] J.-W. Pan and C.-W. Fan, "High luminance hybrid light guide plate for backlight module application," *Opt. Express*, vol. 19, no. 21, pp. 20079–20087, 2011.
[40] J.-W. Pan and Y.-W. Hu, "Design of a hybrid light guiding plate with high luminance for backlight system application," *J. Display Technol.*, vol. 9, no. 12, pp. 965–971, Dec. 2013.
[41] G. Kim, "A PMMA composite as an optical diffuser in a liquid crystal display backlighting unit (BLU)," *Eur. Polym. J.*, vol. 41, no. 8, pp. 1729–1737, 2005.
[42] Y. Hisatake, Y. Kawata, and A. Murayama, "31.3: Viewing angle controllable LCD using variable optical compensator and variable diffuser.," in *SID Symp. Dig. Tech. Papers*, 2005, vol. 36, no. 1, pp. 1218–1221.
[43] H. Kuo, M. Chuang, and C. Lin, "Design correlations for the optical performance of the particle-diffusing bottom diffusers in the LCD backlight unit," *Powder Technol.*, vol. 192, no. 1, pp. 116–121, 2009.
[44] M. Tjahjadi *et al.*, "Advances in LCD backlight film and plate technology," *Inf. Display*, vol. 22, no. 10, pp. 22–27, 2006.
[45] B.-R. Yang *et al.*, "Volumetric scattering layer for flexible transflective display," *Jpn. J. Appl. Phys.*, vol. 47, no. 2R, pp. 1016–1018, 2008.
[46] Y. Asaoka *et al.*, "4.1: Distinguished paper: Cavity shape control of the roll-to-roll fabricated novel microstructure film for improving the viewing-angle characteristics of LCDs.," in *SID Symp. Dig. Tech.Papers*, 2014, vol. 45, no. 1, pp. 17–20.
[47] E. Yamamoto, H. Yui, and S. Katsuta *et al.*, "29.2: Distinguished paper: Wide viewing LCDs using novel microstructure film.," in *SID Symp. Dig. Tech. Papers*, 2014, vol. 45, no. 1, pp. 385–388.
[48] G. Hay, K. P. Capaldo, G. Cojocariu, K. A. Kumar, T. L. Hoeks, T. M. Loehr, J. F. Graf, N. D. Hoffman, S. Leslie, A. Ghosal, and P. Schottland, "Diffuser for flat panel display," U.S. 7 314 652, Jan. 1, 2008, et al..
[49] C.-C. Chen *et al.*, "Thermal deformation of micro-structure diffuser plate in LED backlight unit," *Conf. proc. Soc. Experim. Mechanics Series*, vol. 8, Residual Stress, Thermomechanics & Infrared Imaging, Hybrid Techniques and Inverse Problems, pp. 67–77, 2014.
[50] L. Mingyan, W. Daming, and Z. Yajun *et al.*, "Optimization and design of LCD diffuser plate with micro-semisphere structure," *Procedia Eng.*, vol. 16, pp. 306–311, 2011.
[51] T. R. Sales *et al.*, "LED illumination control and color mixing with engineered diffusers.," in *Opt. Sci. Tec., SPIE 49th Annu. Meeting*, 2004, pp. 133–140.
[52] G. M. Morris, T. R. Sales, and S. Chakmakjian *et al.*, RPC Photonics, "Engineered diffusers™ for display and illumination systems: Design, fabrication, applications," 2007 [Online]. Available: www.physics.uci.edu/isis/Yountville/Sales [Online]. Available: www.RPCphotonics.com
[53] H.-P. D. Shieh, Y.-P. Huang, and K.-W. Chien, "Micro-optics for liquid crystal displays applications," *J. Display Technol.*, vol. 1, no. 1, pp. 62–76, Mar. 2005.
[54] T. R. M. Sales, "Engineered Microlens Diffusers," in *Laser Beam Shaping: Theory and Techniques*. Boca raton, FL, USA: CRC Press, 2014, pp. 367–399.
[55] N. F. Borrelli and D. L. Morse, "Microlens arrays produced by a photolytic technique," *Appl. Opt.*, vol. 27, no. 3, pp. 476–479, 1988.
[56] S. Scheiding *et al.*, "Freeform manufacturing of a microoptical lens array on a steep curved substrate by use of a voice coil fast tool servo," *Opt. Express*, vol. 19, no. 24, pp. 23938–23951, 2011.
[57] R. C. Allen, L. W. Carlson, A. J. Ouderkirk, M. F. Weber, A. L. Kotz, T. J. Nevitt, C. A. Stover, and B. Majumdar, "Brightness enhancement film," U.S. Patent 6111696 A, Aug. 29, 2000.
[58] B. Y. Joo and D. H. Shin, "Design guidance of backlight optic for improvement of the brightness in the conventional edge-lit LCD backlight," *Displays*, vol. 31, no. 2, pp. 87–92, 2010.
[59] Y. H. Jun *et al.*, "Study on the simulation model for the optimization of optical structures of edge-lit backlight for LCD applications," *J. Opt. Soc. Kor.*, vol. 12, no. 1, pp. 25–30, 2008.
[60] M. Schadt and W. Helfich, "Voltage-dependent optical activity of a twisted nematic liquid crystal," *Appl. Phys. Lett.*, vol. 18, no. 4, pp. 127–128, 1971.
[61] M. F. Schiekel and K. Fahrenschon, "Deformation of nematic liquid crystals with vertical orientation in electric fields," *Appl. Phys. Lett.*, vol. 19, no. 10, pp. 391–393, 1971.
[62] R. A. Soref, "Transverse field effects in nematic liquid crystals," *Appl. Phys. Lett.*, vol. 22, no. 4, pp. 165–166, 1973.
[63] S. H. Lee, S. L. Lee, and H. Y. Kim, "Electro-optic characteristics and switching principle of a nematic liquid crystal cell controlled by fringe-field switching," *Appl. Phys. Lett.*, vol. 73, pp. 2881–2883, 1998.
[64] H. J. Yun *et al.*, "Achieving high light efficiency and fast response time in fringe field switching mode using a liquid crystal with negative dielectric anisotropy," *Liq. Cryst.*, vol. 39, no. 9, pp. 1141–1148, 2012.
[65] Y. Chen, Z. Luo, F. Peng, and S.-T. Wu, "Fringe-field switching with a negative dielectric anisotropy liquid crystal," *J. Display Technol.*, vol. 9, no. 2, pp. 74–77, Feb. 2013.
[66] Y. Chen *et al.*, "High performance negative dielectric anisotropy liquid crystals for display applications," *Crystals*, vol. 3, no. 3, pp. 483–503, 2013.

Yating Gao received the B.S. degree in physics from University of Science and Technology of China, Hefei, China, in 2013, and is currently working toward the Ph.D. degree in the College of Optics and Photonics, University of Central Florida, Orlando, FL, USA. Her current research focuses on optical system design in liquid crystal display devices, including backlight module design, optical film design, and quantum dot enhanced LCD.

Ms. Gao currently serves as the Vice President of IEEE Photonics Society Student Chapter at UCF.

Zhenyue Luo received the B.S. and M.S. degrees in optics from Zhejiang University, Hangzhou, China, in 2007 and 2010, respectively.

Since 2010, he has been a research assist ant in Photonics and Display Group, University of Central Florida, Orlando, FL, USA. His current research focuses on backlight design and liquid crystal devices.

Ruidong Zhu, photograph and biography not available at time of publication.

Qi Hong, photograph and biography not available at time of publication.

Shin-Tson Wu (M'98–SM'99–F'04) received the B.S. degree in physics from National Taiwan University, Taipei, Taiwan, and the Ph.D. degree from the University of Southern California, Los Angeles, CA, USA.

He is a Pegasus professor at College of Optics and Photonics, University of Central Florida, Orlando, Orlando, FL, USA.

Dr. Wu is the recipient of the OSA Esther Hoffman Beller Medal (2014), SID Slottow–Owaki prize (2011), OSA Joseph Fraunhofer award (2010), SPIE G. G. Stokes award (2008), and SID Jan Rajchman prize (2008). .He is a Charter Fellow of the National Academy of Inventors, a Fellow of the Society of Information Display (SID), Optical Society of America (OSA), and SPIE. He is the founding Editor-in-Chief of IEEE/OSA JOURNAL OF DISPLAY TECHNOLOGY

Ming-Chun Li, photograph and biography not available at time of publication.

Seok-Lyul Lee, photograph and biography not available at time of publication.

Wen-Ching Tsai, photograph and biography not available at time of publication.